Saudi Pharmaceutical Journal 31 (2023) 101692

HOSTED BY

Contents lists available at ScienceDirect

Saudi Pharmaceutical Journal

journal homepage: www.sciencedirect.com

Original article

Lomustine's nanoemulsion as nose-to-brain drug delivery system for CNS tumor treatment

Maryam H. Alaayedi [a,*], Nidhal K. Maraie [b]

[a] Department of Pharmaceutics, College of Pharmacy, Mustansiriyah University, Iraq
[b] Department of Pharmaceutics, College of Pharmacy, Al-Farahidi University, Iraq

ARTICLE INFO

Article history:
Received 11 May 2023
Accepted 23 June 2023
Available online 28 June 2023

Keywords:
Lomustine
Brain tumor
Nanoemulsion
Oil
Surfactant
Co-surfactant

ABSTRACT

Nose-to-brain delivery allows the direct targeting of drug molecules bypassing the Blood Brain Barrier and systemic effect. Nanoemulsion is one of the novel strategies to deliver drug in this route due to its simplicity in manufacturing, long-term stability, and strong solubilization property for drug. The anti-cancer drug lomustine had poor oral bioavailability in addition to its serious side effect, therefore, developing more effective drug delivery with direct targeting towards the brain through intra-nasal administration applying nanoemulsion technology is a promising alternative. The work involved lomustine solubility screening in oils, surfactants and cosurfactants as well as emulsifier ratio (Smix) nanoemulsion area was identified using pseudo-ternary phase diagrams. Eighteen nanoemulsion formulas were produced for optimization, then characterized for droplet size, polydispersity index, zeta potential, entrapment efficiency, conductivity, transmittance, dilution, visual transparency, physical stability and in vitro release. The optimum NE formula showed droplet size, zeta potential, polydispersity index, entrapment efficiency, %transmittance, conductivity of 31.31 nm, −30.65 mV, 0.159, 98.12%, 99.08%, and 951 us/cm, respectively. The best formula released 100% lomustine within 15 min which is a promising potential drug delivery system that may deliver the drug quickly and directly to the brain as a safe and effective alternative to oral delivery.

1. Introduction

Glioblastoma Multiforme (GBM) is considered as highly aggressive, has less than 5% five-year survival rate, and it can happen at any age but more often in elderly. This cancer is characterized by infiltration, significant angiogenesis and uncontrolled cell proliferation. Therefore, the most active cancer chemotherapy available such as oral or parenteral can slightly enhance the survival rate (Hanif et al., 2017). Hence, strategies to increase the chemotherapeutic agents' localization to the brain tumor are required to decline the rate of fatality (Lundy et al., 2021).

The typical therapeutic approach for chemotherapeutics is to provide them peripherally (parenterally or orally); however, these delivery routes degrade the drug molecule's potency, resulting in poor brain targeting effectiveness. The bioavailability of medications when taken orally can also be impacted by the first-pass effect, systemic clearance, enzymatic degradation, plasma protein binding, and volume of distribution. Intranasal administration (IN) permits a quicker delivery method. Direct administration from the nose to the brain has the advantages of a rapid onset of action, better targetability as well as reduced systemic toxicity, and elimination. Additionally, by using this route and avoiding first pass metabolism, a higher concentration of the active pharmaceutical ingredient (API) can be reached in the CNS (Islam et al., 2020).

Nasal mucus modulates permeability by impeding the transit of particles (>200 nm) over the mucosal epithelia. It is a selective barrier with a thickness of 5–15 μm and pore size of 50–150 nm. Particles that fulfill the particle size requirement can absorb through a variety of channels. Tight junctions allow for extracellular nasal transport, however only free molecules can enter via this small opening (3.9–8.4°A). Particles smaller than 20 nm are therefore more likely to achieve this kind of extracellular transport from the nasal cavity to the brain. As a result, the concentration,

* Corresponding author.
E-mail addresses: maryamalaayedi@uomustansiriyah.edu.iq (M.H. Alaayedi), drnidhalkhazaal@uoalfarahidi.edu.iq (N.K. Maraie).

Peer review under responsibility of King Saud University.

Production and hosting by Elsevier

https://doi.org/10.1016/j.jsps.2023.06.025
1319-0164/

lipophilicity, and particle properties of the nanoparticles have a significant impact on their ability to be internalized (Lai et al., 2009). Nanoemulsion (NE) is one of the strategies which achieve this goal. The advantages of nanoemulsions include eliminating variability in absorption, increasing the rate of absorption, aiding in the solubilization of lipophilic drugs, providing aqueous dosage forms for drugs that are not water soluble and increasing bioavailability (Ganta et al., 2014).

Lomustine is alkylating chemotherapy that used for GBM treatment. It is considered as nonselective for cancerous cells and affect the rapid dividing cells (normal and abnormal). Therefore, reducing the lomustine side effects and toxicity requires drug dose lowering; however, cancer cells require high enough dose to be killed. Lomustine is absorbed orally and can penetrate the lipophilic membrane due to its lipophilicity. After its absorption, it undergo extensive metabolism in liver with a half-life of 94 min (Chen et al., 2013; Gustafson and Page, 2013).

The work's aim is to prepare lomustine as nanoemulsion to be a platform for targeting brain cancer intranasally in order to improve solubility, avoiding first pass drug metabolism and reduce systemic side effect of this chemotherapeutic agent as well as evaluate the contribution of intranasal formulation on the in vitro characteristics of the drug.

2. Materials and methods

2.1. Materials

Lomustine and Capryol 90 was purchased from Aladdin, China. Span 20, 40, 80, Tween 20, 40, 60, 80, PEG 200, 400, propylene glycol and methyl orange were bought from Himedia Laboratories Pvt. Ltd. (India). Oleic acid was purchased from Central Drug House (P) Ltd. (CDH®), New Delhi (India). Olive oil was from Central Drug House (P) Ltd. Castor, and eucalyptus oils, almond oil and cod liver oil were from Wuhan Senwayer Century Chemical Co., Ltd, China. Tricetin from Quzhou Rundong Chemical Co., Ltd., China. Cromophor EL and transcutol P were from Shanghai Ruizheng chemical Tech Co., Ltd, China. Labrasol was from Gattefosse, USA. Methanol and cumin oil were purchased from Sigma-Aldrich, USA. Peppermint oil was from BAR-SUR-LOUP, France.

2.2. Methods

2.2.1. Lomustine solubility determination

Lomustine solubility was determined in different oils (Olive oil, Cumin oil, Oleic oil, Tricetin, Eucalyptus oil, Peppermint oil, Almond oil and Cod liver oil and emulsifiers (Labrasol, Triton X-100, Triton X-114, Span 20, Span 80, Tween 20, Tween 80, PEG 200, PEG 400, Capryol 90, Propylene glycol, Transcutol and Cremophore EL). An access amount of the drug was added to 5 ml of each liquid medium placed in capped glass vial and put on magnetic stirrer for continuous stirring (about 500 rpm) for 48 h at room temperature (25 °C) to reach equilibrium. Each equilibrated sample was filtered via syringe filter (0.45 μm) and then diluted with appropriate volume of methanol. The drug solubility was determined via spectrophotometer at its λmax (Shukla et al., 2016).

2.2.2. Pseudo-ternary phase diagram construction

The construction of pseudo-ternary phase diagram was determined using aqueous titration method. The selected best solubilizing oil, and emulsifiers were used (eucalyptus oil, triton X-100 as a surfactant as well as cremophore and transcutol P as co-surfactants). The diagrams were drawn to evaluate the appropriate ratios of Smix depend on the emulsion (monophasic) area that formed. Range of different ratios of Smix were (4:1, 3:1, 2:1, 1:1, 1:2, 1:3, 1:4) and for the oil to Smix ratios were between 1:9 to 9:1 to get the boundaries of the emulsion area. Each ratio mixture of oil and Smix was titrated against water and observed optically. The amount of water that results in transition from transparency to turbidity is considered as end point of titration. The biphasic samples must be excluded from the diagram when there is separation of the phases after the turbidity appears. The monophasic samples must be drawn in the diagram when the liquids are clear and transparent. The area of the emulsion is that covered by only the monophasic liquid points. The same procedure repeated with other stated Smix ratios. The constructed diagrams were drawn with "Ternary Plot Generator". The larger emulsion area means the greater capacity of hydration and was selected as the best composition of emulsion (Gurpreet and Singh, 2018).

2.2.3. Preparation of lomustine nanoemulsion

Lomustine o/w NE formulas were prepared according to the results of the pseudo-ternary diagrams. First, the drug was solubilized in oil and Smix mixture using magnetic stirrer, then the water added drop by drop on magnetic stirrer (~500 rpm) at room temperature until clear formula prepared. The volume of each formula 25 ml where each 200 μl containing 5 mg drug. The formulas were then subjected to ultrasonic force using probe sonicator at 20 KHz and 200w (Qsonica sonicator; USA) for 5 min to reduce the NE droplet size, sonication lead to heat generation and this problem resolved by putting the formula into iced bath (Delmas et al., 2011; Ghosh et al., 2013). The prepared formulations composition shown in the Table 1 below.

2.2.4. Characterization of lomustine NE

2.2.4.1. Visual transparency. The transparency of the prepared NE (F1-F18) was determined optically by placing the formulas in transparent clear glass vials using good light source (Hussein, 2014).

2.2.4.2. Determination of droplet size, poly dispersity index (PDI) and zeta potential. The determination of the mean droplet size, zeta (ʒ) potential (droplet charge) and PDI (size range of droplet; particles) utilizing dynamic light scattering technique (Malvern Zetasizer Nano ZS). In this technique, the fluctuations of scattered light were analyzed because of Brownian motion of the NE particles in the formulations. The viscosity of the oil and surfactants was reduced via dilution of the formulas with double distilled water with agitation. Then, one milliliter of the each resulted diluted NE formula was injected into the folded capillary zeta cell at 22 °C (173°angle) and monitor the light scattering. Finally, the average droplet size, PDI and ʒ-potential were recorded (Li et al., 2011; Sharma et al., 2020).

2.2.4.3. Entrapment efficiency (EE). This test was performed to determine the drug content in each formula of NE. Lomustine content in NE formulation was determined using UV-scpectroscopic method. One milliliter of each formula was first solubilized with 70 ml methanol then sonicated for 30 min in 100 ml capacity volumetric flask. The volume completed to 100 ml with methanol, then centrifuged at room temperature at 3500 rpm for 20 min. The resulted transparent supernatant layer was taken and evaluated for drug spectroscopically (Shimadzu, Japan) at the drug UV lambda max (Deore et al., 2019).

$$EE = \frac{drug\ \ content\ \ in\ \ the\ \ product\ \ obtained\ \ (mg)}{total\ \ amount\ \ of\ \ drug\ \ added\ \ (mg)} 100$$

2.2.4.4. Dye solubilization test. This test was performed by mixing 2 mg/ml of the dye (methyl orange solution; water soluble dye) with each formula and observing visually whether the dye color

Table 1
The composition of lomustine NE formulas.

Formulas Code	Drug (mg)	Eucalyptus Oil % v/v	Smix type (Surfactant: Co-surfactant)	Smix Ratio	Smix %v/v	Water to achieve 200 µl
F1	5	10	Triton X-100: Cremophore El	3:1	40	QS
F2	5	10	Triton X-100: Cremophore El	3:1	30	QS
F3	5	10	Triton X-100: Cremophore El	2:1	50	QS
F4	5	10	Triton X-100: Cremophore El	2:1	30	QS
F5	5	10	Triton X-100: Transcutol P	3:1	60	QS
F6	5	10	Triton X-100: Transcutol P	3:1	30	QS
F7	5	10	Triton X-100: Transcutol P	2:1	60	QS
F8	5	10	Triton X-100: Transcutol P	2:1	50	QS
F9	5	10	Triton X-100: Transcutol P	2:1	40	QS
F10	5	5	Triton X-100: Cremophore El	3:1	30	QS
F11	5	5	Triton X-100: Cremophore El	2:1	30	QS
F12	5	5	Triton X-100: Transcutol P	3:1	60	QS
F13	5	5	Triton X-100: Transcutol P	3:1	50	QS
F14	5	5	Triton X-100: Transcutol P	3:1	40	QS
F15	5	5	Triton X-100: Transcutol P	3:1	30	QS
F16	5	5	Triton X-100: Transcutol P	2:1	60	QS
F17	5	5	Triton X-100: Transcutol P	2:1	50	QS
F18	5	5	Triton X-100: Transcutol P	2:1	40	QS

spread evenly (o/w nanoemulsion) or not (w/o nanoemulsion) via the external continuous phase, this test was used to determine the nature of continuous phase for each prepared lomustine NE (Ashoor and Ghareeb).

2.2.4.5. Conductivity test. Measurement of electrical conductivity (σ) of the NE formulations was determined using conductometer (Hanna instruments; USA) via insertion of the instrument probe in 10 ml of the NE formula at room temperature. The recorded result in µs/cm. This test had been used to determine the nature of the NE if it is o/w or w/o. If the NE conduct electricity then the external phase is water, the NE is o/w since water is electrical conductor (highly conducting than oil) and vise versa (Chaudhari and Kuchekar, 2018).

2.2.4.6. Dilution test (dispersity test). This test was carried out in order to check the NE physical stability. It is done by diluting 1 ml of each formulation to 50 ml, 100 ml and 500 ml using distilled water at 37 °C with stirring constantly at 50 rpm. The formulas were observed visually for turbidity, clarity and phase separation (Abdulkarim et al., 2010).

2.2.4.7. Transmittance percentage (%T; turbidity test). This test was applied to determine the transparency of the formatted NE. Turbidity test was performed by taking 2 ml of NE and measuring the absorbance at UV–Vis spectrophotometer at 650 nm using distilled water as blank. The percent of transmitted light (%T) was obtained using the equation below:

$$A = 2 - log\%T$$

where, A is absorbance and %T is transmittance percentage (Prajapati et al., 2015).

2.2.4.8. pH determination. pH determination of each NE formulas was done using pH meter (Hanna instruments; USA) to ensure the compatibility of the formulas with the nasal cavity pH.

2.2.4.9. Viscosity. The prepared NE viscosity was measured by using viscometer (ATAGO's viscosity meter VISCO™; Japan). Spindle A1 (for moderate to high viscosity formulas) and UL (for formulas with low viscosity < 50 mPa.s) was used.

2.2.4.10. Physical stability studies of nanoemulsion. **Centrifugation test:** All the formulas were subjected to centrifugation using centrifuge (Fanem, 206-R Centrifuge, Brazil) with 3500 rpm for 30 min. when the formulas that pass this test (maintaining a homogeneity state) were considered stable and pass to the next below tests (Ghosh et al., 2013).

Heating/cooling cycle test: This test was performed to evaluate the stability of nanoemulsions at extreme temperature changes. Six refrigeration cycles of at 4 °C and 45 °C with oven temperature for 48 h for each temperature. Each formula was subjected for heating and cooling cycle by putting the formula 2 d in refrigerator at 4 °C then 2 d in oven at 45 °C. This successive cycles repeated six times (Mota Ferreira et al., 2016).

Freeze/ thaw cycle: The formulas were left in deep freezer (at −20 °C) for one day, then they were taken out and kept at 25 °C. The stable NE should return to original form within 2–3 min. Each formula was subjected to two cycles (Ankith et al., 2013).

2.2.4.11. In-vitro drug release study. Lomustine release was studied through dialysis membrane (MWCO 12000 Da). The in vitro drug release from all produced NE formulas (F1-F18) was assessed using rotating paddle dissolution device type. The 200 µl of NE (containing 5 mg of lomustine) in the sealed dialysis bag was immersed at a speed of 50 rpm in 200 ml of phosphate buffer saline media (PBS; pH 6.4). The medium's temperature was preconditioned to 34 °C. At intervals of 5, 15, 30, 45, 60, 90, 120, 150, 180, 240, and 360 min, 2 ml aliquots are removed and immediately replaced with fresh dissolving medium. A UV–Vis spectrophotometer was used to measure the drug concentration in the withdrawn sample at the chosen λmax (Raavi et al., 2014).

2.2.4.12. Selection of optimum NE formula. Suitable droplet size, droplet size distribution, PDI, zeta potential, electroconductivity, transmittance percentage, pH, viscosity, in vitro release are the factors that went into choosing the best formula.

2.2.4.13. Nanoemulsion morphology determination by TEM. A transmission electron microscope running at 30 KV was used to better describe the selected NE formula. Where a drop of diluted optimized formula was allowed to deposit on the 300 mesh circular formvar-stained copper film grid and allowed to dry. After the slide had dried completely, it was examined under a microscope to evaluate the droplets' size and shape (Klang et al., 2012).

2.2.4.14. Lomustine and excipients compatibility determination using Fourier transform infrared spectroscopy (FTIR). The liquid cell was used to acquire the FTIR spectra of samples of the NE optimized

formula composition in contrast to pure medication (Shimadzu, Japan). This was done by pouring few drops of the sample onto a NaCl or KBr aperture plate and sandwiching it under another aperture plate, ensuring that no gas bubbles are trapped. By placing spacers between the aperture plates or by correctly tightening the screws, the thickness is changed in accordance with the sample absorbance.

3. Results

3.1. Lomustine solubility study

Lomustine showed high solubility in eucalyptus oil (41.08 ± 0. 023 mg/ml) more than other tested oils. Whereas Triton X-100 was the best solubilizing surfactant and Cremophore EL as well as Transcutol P were the best solubilizing cosurfactants. The lomustine solubility study results is shown in Fig. 1.

3.2. Pseudo-ternary phase diagram construction

The pseudo-ternary phase diagram was constructed using eucalyptus oil and various ratios of Smix (4:1, 3:1, 2:1, 1:1, 1:2, 1:3, 1:4). The best result (largest area of monophasic, NE) was Smix; Triton x-100: Cremophore El 3:1, then 2:1 as explained in Fig. 2.

3.3. Preparation of lomustine nanoemulsion (NE)

Eighteen formulas of NE were prepared using different percentage of eucalyptus oil (5% and 10%), two types of Smix Triton X-100: Cremophore El and Triton X-100: Transcutol P with different Smix percentages (60, 50, 40 and 30%) and different Smix ratios. All the prepared formulas were characterized and evaluated for optimization.

3.4. Lomustine nanoemulsion characterization

3.4.1. Visual transparency

All the prepared NE formulations were optically clear.

3.4.2. Nanoemulsion droplet size, poly dispersity index (PDI) and zeta potential measurement

The average droplet size, PDI and zeta potential of the formulated NE are shown in Table 2. The NE droplet size resulted from the controlling process parameters as the energy input type and time of emulsification as well as dependency on the amount of Smix and dispersed phase concentration (Delmas et al., 2011). The particle size of the formulated NE was less than 100 nm. PDI for all the formulated NE were of (0.155–0.288). Zeta potential (ζ) of the produced NE were within −30.65 to 25.63 range.

3.4.3. Drug entrapment efficacy

The drug EE results shown in Table 2. The EE was found to be high (94.88% and more) in all the prepared NE formulations.

3.4.4. Dye solubility test

All the NE formulations were colored orange homogenously by the dye.

3.4.5. Conductivity test

The electrical conductivity of all NE formulas was high (241–9 98 µs/cm), as shown in Table 3.

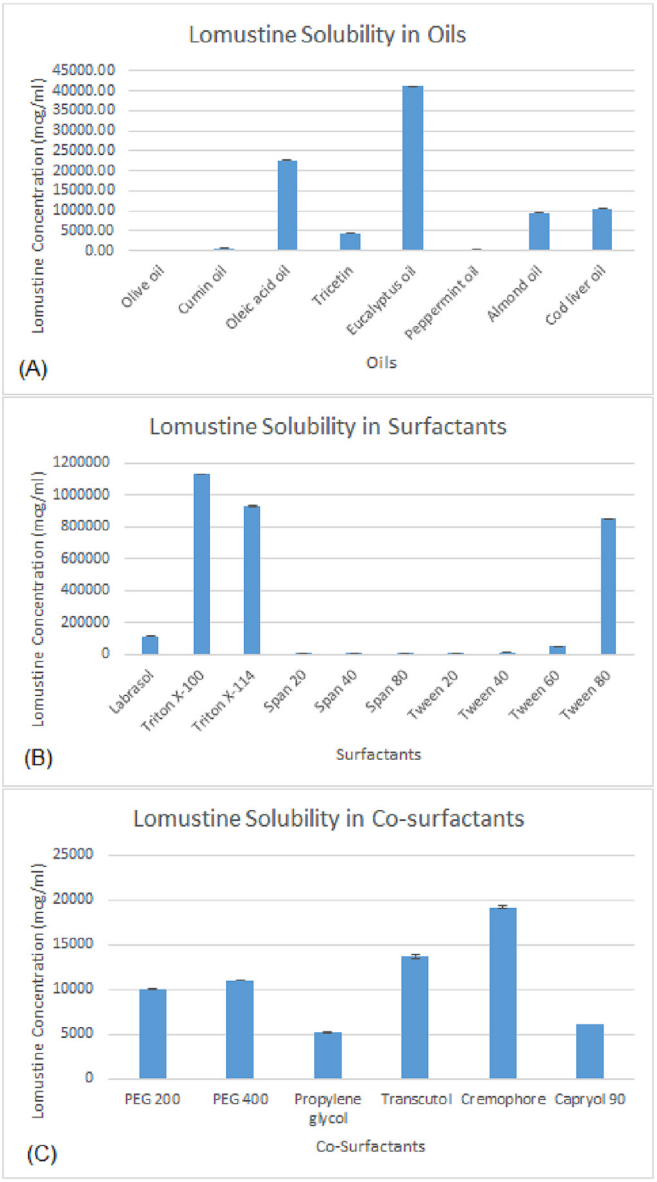

Fig. 1. Lomustine's solubility study in (A) oils, (B) surfactants, and (C) co-surfactants. All results represent mean concentration of the drug (in µg/ml) ± SD. (n = 2).

3.4.6. Dilution test (dispersity test)

The results demonstrated that upon addition of water (continuous phase), all the 18 formulas showed clear NE in less than 60 sec without any precipitation or cracking.

3.4.7. Transmittance percentage (%T; turbidity test)

All of the prepared NEs formulas were clear, transparent, and easily transmit light, as seen by values of the percentage transmittance that were closer to 100%. (Table 3).

3.4.8. pH determination

All the pH values of the produced NE was within range of 3.35–5.12, as shown in Table 3.

3.4.9. Viscosity measurement

The formulas (F5-F9 and F12-F18) that containing Transcutol P as a co-surfactant in Smix mixture showed the lowest viscosity.

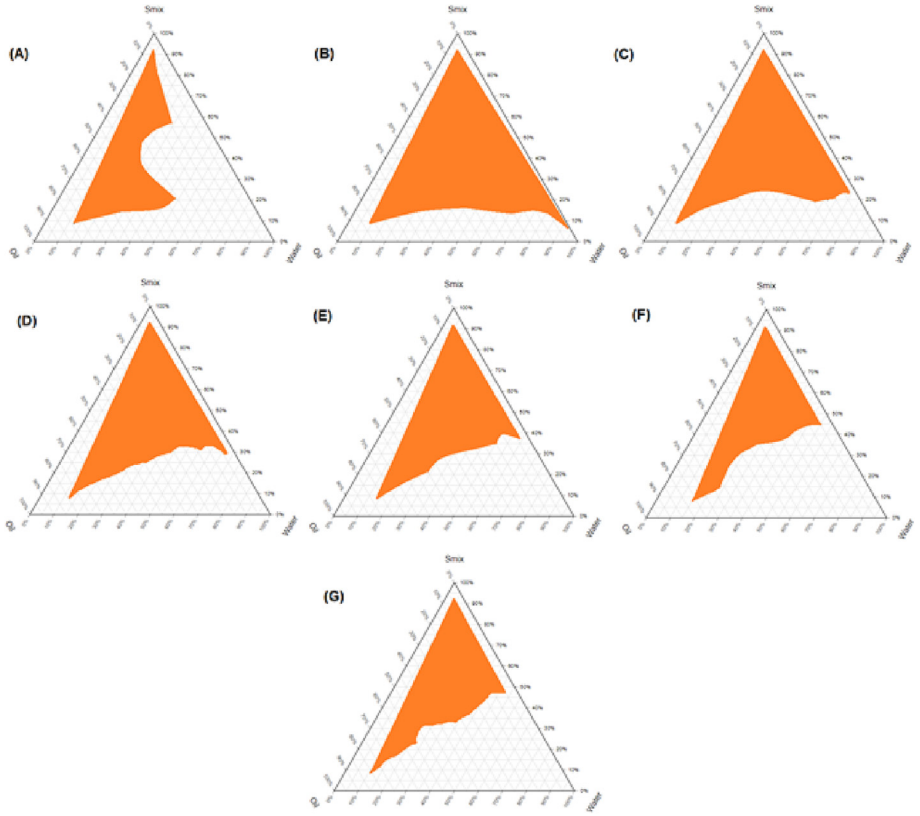

Fig. 2. The triangular co-ordinate of o/w emulsion diagram using eucalyptus oil, Smix (Triton X-100: Cremophore El) in different ratios, where (A) 4:1, (B) 3:1, (C) 2:1, (D) 1:1, (E) 1:2, (F) 1:3, and (H) 1:4, and DDW.

Table 2
Mean droplet size, PDI, zeta potential and Entrapment efficacy of the prepared lomustine NE (n = 3) (mean ± SD).

NE Code	Droplet size ± SD	PDI ± SD	Zeta potential ± SD	EE%± SD
F1	31.31 ± 1.2	0.159 ± 0.02	−30.65 ± 0.3	98.12 ± 2.0
F2	99.12 ± 1.9	0.172 ± 0.01	−25.87 ± 1.1	95.07 ± 3.2
F3	87.44 ± 2.2	0.241 ± 0.04	−28.55 ± 1.3	94.98 ± 2.4
F4	98.86 ± 4.3	0.223 ± 0.02	−25.63 ± 2.2	98.43 ± 1.9
F5	11.32 ± 0.8	0.239 ± 0.03	−29.02 ± 1.4	99.72 ± 2.9
F6	14.4 ± 0.5	0.238 ± 0.04	−28.54 ± 2.3	98.66 ± 1.7
F7	10.99 ± 0.2	0.164 ± 0.01	−31.55 ± 2.1	96.77 ± 2.8
F8	12.7 ± 0.3	0.288 ± 0.04	−30.76 ± 0.4	95.98 ± 1.2
F9	13.05 ± 0.1	0.262 ± 0.02	−30.42 ± 2.3	96.97 ± 1.7
F10	78 ± 2.3	0.182 ± 0.01	−29.98 ± 0.4	99.72 ± 2.5
F11	43.48 ± 2.6	0.155 ± 0.01	−30.51 ± 2.4	99.72 ± 2.3
F12	94.86 ± 3.1	0.209 ± 0.03	−31.63 ± 2.0	98.43 ± 2.6
F13	73.7 ± 4.1	0.203 ± 0.04	−31.53 ± 3.1	98.13 ± 3.2
F14	13.93 ± 0.4	0.224 ± 0.03	−29.4 ± 1.8	96.92 ± 3.3
F15	66.2 ± 2.8	0.188 ± 0.01	−28.89 ± 2.5	97.01 ± 2.6
F16	10.78 ± 0.1	0.278 ± 0.02	−32.68 ± 3.1	97.33 ± 2.2
F17	9.96 ± 0.3	0.196 ± 0.04	−31.88 ± 3.3	96.43 ± 1.3
F18	10.81 ± 0.1	0.213 ± 0.01	−31.45 ± 4.2	97.88 ± 2.1

Formulas F9 (containing 40% Triton X-100:Transcutol P Smix in 2:1 ratio) has lowest viscosity between the others. The highest viscosity was observed with formulas that containing Cremophore El (F1-F4, F10 and F11), formula F1 (containing 40% Triton X-100: Cremophore El Smix in 3:1 ratio) and F3 (containing 50% Triton X-100:Cremophore El Smix in 2:1 ratio) showed highest viscosity. The viscosity of the prepared NE was show in Table 3.

3.4.10. Physical stability studies of nanoemulsion

All NE formulas had passed successfully the physical tests under different stress conditions (centrifugation, heating/cooling, and freeze/thaw cycle) with no separation and creaming (Shaikh et al., 2019).

3.4.11. In vitro release study

Fig. 3 shows the efficacy of different variables on the release pattern of the prepared NE formulas (F1-F18). Fig. 3A shows the effect of using different amount of oil on drug release. Fig. 3B shows the effect of co-surfactant type. While, Fig. 3C shows the effect of Smix percentage on drug release. Fig. 3D shows the effect of Smix ratio on drug release. Fig. 4 shows the rest formulas that mainly their drug release affected by viscosity.

Table 3
Electrical conductivity measurements, transmittance percentage of lomustine NE formulas (n = 3) (mean ± SD).

Formula Code	Electrical conductivity (µs/cm) ± SD	Transmittance (%T) ± SD	pH value ± SD	Viscosity (mPa.s) ± SD
F1	951 ± 2.0	99.08 ± 0.02	5.12 ± 0.10	568 ± 3.2
F2	980 ± 5.0	99.54 ± 0.01	4.44 ± 0.20	513 ± 4.1
F3	314 ± 3.0	99.03 ± 0.01	4.56 ± 0.11	590.9 ± 11.2
F4	990 ± 2.0	99.54 ± 0.02	4.19 ± 0.01	574.3 ± 2.8
F5	417 ± 5.0	99.47 ± 0.03	3.89 ± 0.20	112.8 ± 1.4
F6	743 ± 2.0	99.68 ± 0.02	3.4 ± 0.120	30.1 ± 1.2
F7	252 ± 4.0	99.58 ± 0.01	3.95 ± 0 03	66 ± 2.4
F8	380 ± 3.0	99.72 ± 0.01	3.64 ± 0.04	60.9 ± 3.1
F9	526 ± 6.0	99.77 ± 0.02	3.43 ± 0.13	23.6 ± 2.5
F10	874 ± 6.0	99.56 ± 0.02	4.34 ± 0.15	510 ± 2.2
F11	911 ± 7.0	99.56 ± 0.01	4.28 ± 0.14	573 ± 3.3
F12	520 ± 3.0	99.52 ± 0.03	3.85 ± 0.05	110.9 ± 2.7
F13	950 ± 7.0	99.58 ± 0.02	3.63 ± 0.11	101.3 ± 4.2
F14	995 ± 5.0	99.63 ± 0.01	3.54 ± 0.02	56.8 ± 3.0
F15	998 ± 1.0	99.70 ± 0.02	3.35 ± 0.15	26.3 ± 1.1
F16	241 ± 1.0	99.61 ± 0.01	3.84 ± 0.03	65.1 ± 3.1
F17	341 ± 3.0	99.75 ± 0.01	3.63 ± 0.01	61.1 ± 2.5
F18	533 ± 5.0	99.79 ± 0.03	3.37 ± 0.07	32.6 ± 1.0

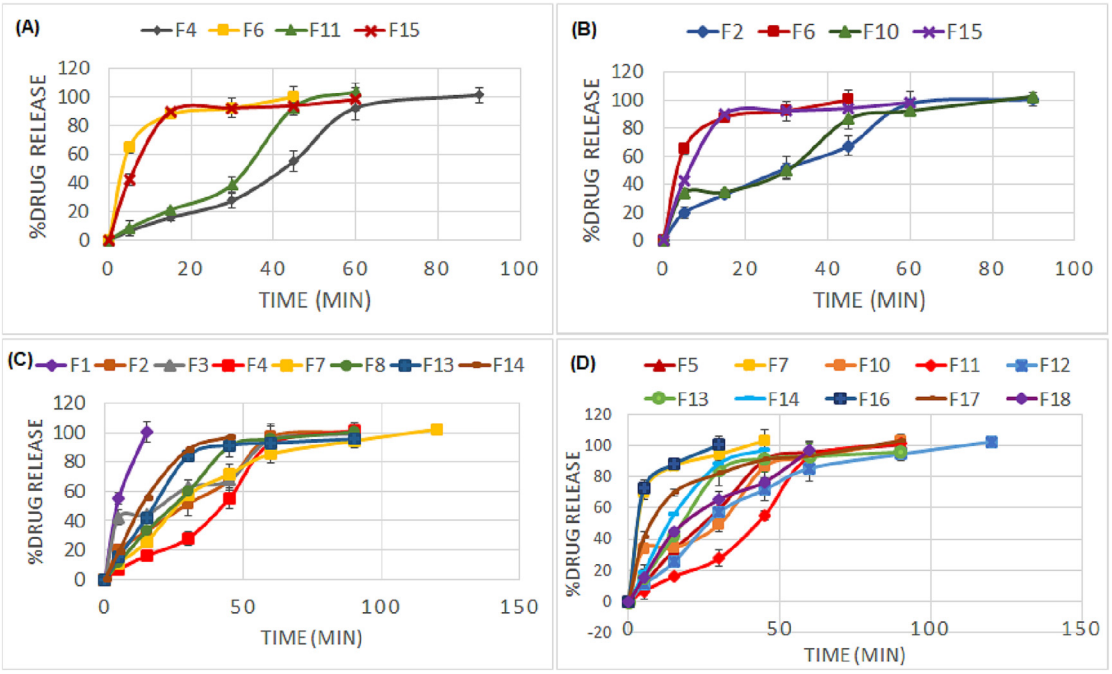

Fig. 3. In vitro lomustine release study from NE using PBS 200 ml for 6 h for the eighteen formulas, where (A) explain the effect of using different amount of oil on drug release, (B) explain the effect of co-surfactant type, (C) explain the effect of Smix percentage on drug release and (D) show the effect of Smix ratio on drug release. (n = 3) (mean ± SD).

3.4.12. Selection of the best formula

Based on the results obtained, formula F1 was selected as the best lomustine nanoemulsion formula.

3.4.13. Determination of optimized nanoemulsion formula morphology by TEM

The morphology of the optimum nanoemulsion formula (F1) was characterized by transmission electron microscopy (Malik et al., 2022) (Fig. 5). The images shows dark globules with bright surrounding, with average droplet size (31.31 nm).

3.4.14. Lomustine and excipients compatibility determination using FTIR

Fig. 6 showed no significant differences in position and shape of the FTIR absorption peaks between the pure lomustine and the optimum NE formula composition diagram. Lomustine pure powder showed peaks at 3348 cm^{-1} for NH, 1702 cm^{-1} for carbonyl group, about 1500 cm^{-1} for nitrozo group. In addition, peaks at 1450 and 1486 cm^{-1}, 2857 and 2933 cm^{-1} for aliphatic CH stretching (symmetric and asymmetric).

4. Discussion

4.1. Lomustine solubility study

The best solubilizing surfactant was Triton X-100 which is non-ionic surfactant containing hydrocarbon lipophilic group and its HLB value of 13.5 (required to produce o/w) (Egan, 1976). Whereas, the best solubility of lomustine was in co-surfactants Cremophore EL and Transcutol P. Cremophore EL is hydrophobic in nature and it

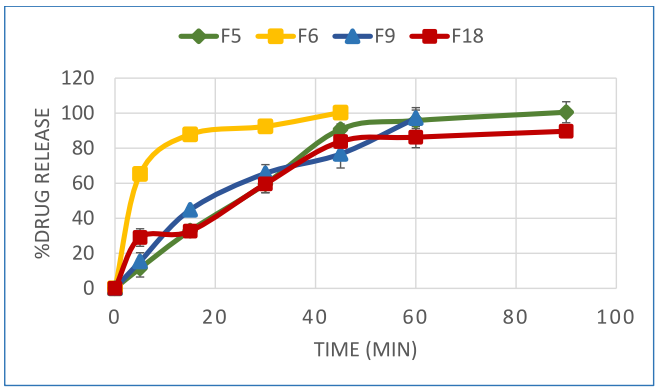

Fig. 4. The effect of viscosity on drug release. (n = 3) (mean ± SD).

is used as formulation vehicle to enhance the solubility of different poor water soluble medications involving anticancers such as pactitaxel (Nan, 2015). Transcutol P (diethylene glycol monoethyl ether) is highly pure solvent and powerful solubilizer used to enhance the solubility and dissolution of many drugs (Al-Tamimi and Hussein, 2021).

4.2. Pseudo-ternary phase diagram construction

The oily phases used was eucalyptus oil depending upon the drug solubility study and only small amount of oil was used because as the oil phase increased lead to increase in Smix percent and that could result in nasal irritation (Rosen et al., 2013). The surfactant role is to be adsorbed and stabilized at the oil–water interface in order to form a protective layer or barrier around the dispersed internal droplets in the emulsion, therefore, it stabilizes the emulsion via decreasing the interfacial tension (ɣ) of the mixture (Jin et al., 2021) and could impart a charge on that droplets surface to further improve the system stability and prevent the physical contact between the droplets then coalescence (Khan et al., 2011; Sekeri et al., 2020). Co-surfactant, Cremophore EL (HLB of 15.3) which lead to further reduction in interfacial tension (Zeng et al., 2017). This would increase or enlarge the polar head region and produce o/w NE and give a positive curvature (Mathew and Juang, 2007; Muzaffar et al., 2013). Transcutol P is a solvent with high-purity and good solubilizer for the drug (Józsa et al., 2022).

4.3. Evaluation of lomustine nanoemulsion

The transparency of the prepared formulas might be due to the small droplet size of NE which lead to weak light scatters, indicating the efficiency of the method applied (Çınar, 2017).

The decrease in the %v/v of the dispersed eucalyptus acid oil (F10 containing 5%v/v oil in comparison to F2 contains 10 %v/v oil) keeping same type and Smix ratio (3:1) constant as well as F11 containing 5%v/v oil in comparison to F4 containing 10% v/v oil and both containing same type and Smix ratio (2:1), caused decreasing the droplet size because the reduction in the oil phase percentage makes the Smix concentration sufficient to disperse and stabilize the oil phase in the system (Ali et al., 2014). Similar results observed with Lidocaine NE (Sarheed et al., 2020).

The change of co-surfactant type from Cremophore El (F10 and F2) to Transcutol P (F15 and F6) lead to reduce the droplet size of the NE. F15 NE formula that containing 30% of Triton X-100: Transcutol P (3:1) has significantly ($p \leq 0.05$) smaller droplet size than F10 which containing Cremophore El co-surfactant with same Smix percentage and ratio. This could be due to the lower viscosity of Smix in F15 that allow easier and efficient distribution of Smix around the oil droplet. A similar result was obtained for F6 in comparison with F2 where both of them containing the same percentage of Smix (30%) and ratio (3:1), F6 containing Transcutol P as co-surfactant had significantly ($p \leq 0.05$) smaller droplet size than F2 which containing Cremophore El. Moreover, eucalyptus oil needs optimal HLB value of 9.8 (Orafidiya and Oladimeji, 2002) for the surfactant and co-surfactant mixture to give stable w/o emulsion as Triton X-100 HLB is 13.4, for Cremophore El is 13.5 (Algahtani et al., 2022) and Transcutol P of 4.2 (Shah et al., 2015), therefore Transcutol P with Triton might produce HLB value closer to the required for the oil than Cremophore.

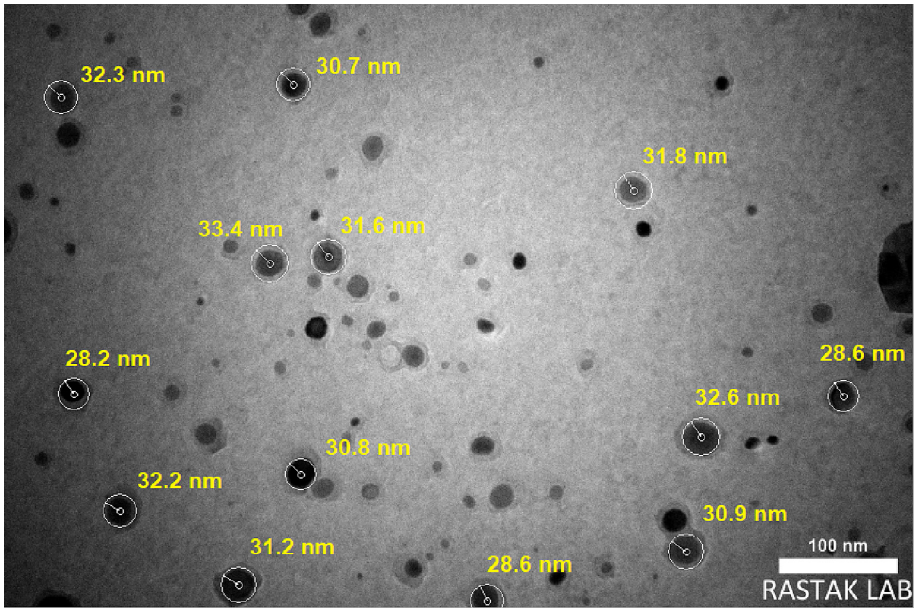

Fig. 5. TEM of F1, the magnifying force is 100kv.

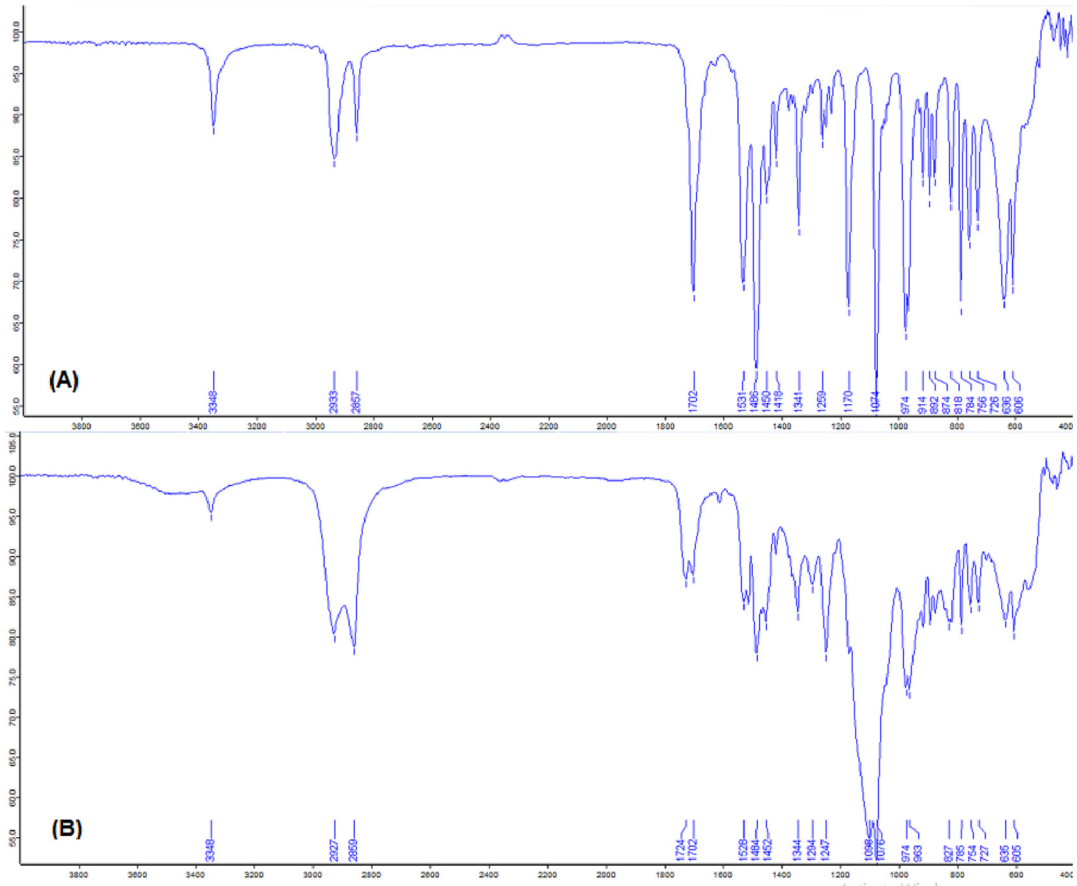

Fig. 6. The FTIR spectra of pure lomustine powder.

The percentage of Smix play an important role in the film formation around the dispersed droplets. Increasing the Smix percentage significantly ($p \leq 0.05$) reduced the particle size of NE, F2 with 30% Smix (3:1 ratio) of 99.12 nm in comparison with F1 of 40% Smix (3:1 ratio) of 31.31 nm as well as F4 of 30% Smix (2:1 ratio) of 98.86 nm with F3 of 50% Smix (2:1 ratio) of 87.44 nm. The surfactant and co-surfactant mixture reduced the interfacial tension at oil/water interface, so it decreases the free energy amount required to disrupt the globules that led to a smaller globules size. A similar results observed with methotrexate nanoemulsion (Jang et al., 2020) and dutasteride nanoemulsion (Ali et al., 2014). However, this scenario did not observed with formulas (F12-F18) contained the Smix of Triton X-100: Transcutol P for both selected ratios (3:1 and 2:1) with oil concentration of 5%. This may be due the small oil amount that might need less Smix to produce smaller size and increasing the percentage of Smix as well as the amount of surfactant ratio may increase the availability of extra free surfactant molecules in the external phase [36]. The fact that the original surfactant concentration was high enough to completely cover the oil droplet and that made F12 with higher Smix (60%) had the larger droplet (94.86 nm). This lead to conclusion that for each oil amount there should be an optimum Smix concentration. Same observation was found with lidocaine NE where the variation in oil amount as well as surfactant affect the penetration in to the hydrophobic zone of the surfactant hence influencing surface curvature and subsequently the droplet size (Gupta et al., 2016; Sarheed et al., 2020).

The change in Smix ratio from 3:1 (F2; 99.12 nm) to 2:1 (F4; 98.86 nm) for Triton X-100: Cremophore El (keeping the percentage of Smix 30%) had no significant ($p > 0.05$) effect on the droplet size change. Where both formulas had 30% Smix and 10% oil. While for formulas (F10 and F11) with oil concentration of 5% and same percentage of Smix (30%), changing the ratio from 3:1 in F10 to 2:1 in F11 significantly ($p \leq 0.05$) reduced the size from 78 nm (F10) to 43.48 nm (F11), reducing the oil amount (5%); the use of 2:1 Smix ratio may give the suitable required HLB that can produce the smaller particle size. Same results observed with lidocaine NE (Ali et al., 2014).

For formulas with Smix of Triton X-100: Transcutol P using 5% oil (F12, F13, F14 and F15 of 3:1 Smix ratio and F16, F17 and F18 of 2:1 Smix ratio), increasing the ratio significantly ($p \leq 0.05$) increased the droplet size, as F18 (2:1) had 10.05 nm while F14 (3:1) had 13.93 nm. A similar result was gained for 60% Smix, when F16 (2:1 ratio) showed smaller size of 10.78 nm and F12 (3:1) of 94.86 nm as well as 50%, where F17 had smaller size than F13 of 9.96 nm and 73.7 nm, respectively. This could be explained on the basis that reducing the Smix ratio enhanced water penetration into oil droplets resulting in breakdown of oil droplets leading to smaller droplets (Pouton, 1997).

It was observed that NE containing Transcutol P generally had significant ($p \leq 0.05$) smaller droplet size than those containing Cremophore El, where F6 (containing Transcutol P in 30% Smix ratio of 3:1) had 14.4 nm in comparison to F2 (containing Cremophore EL in 30% Smix ratio of 3:1) which had 99.12 nm as well as with Transcutol P containing formulas F16, F17 and F18 (in spite of their percentage of Smix) gave small droplet size, as the Transcutol P had low viscosity than Cremophore El, where the high viscous material had difficulty to achieve homogeneity and distribution around the oil droplet. Similar results observed with Oleanolic Acid NE (Xi et al., 2009).

PDI for all the prepared formulas were low value of (0.155–0.288) indicating uniform distribution, homogeneity and high quality of nano-sized droplets preparations. Since PDI of high value of more than 0.7 to 1 is considered to have broad particle size distribution and more than 1 is considered very polydisperse (Patel et al., 2013).

Zeta potential (ζ) is a crucial metric that provides insight into the system. The difference in potential between the densely bonded area's surface and the electro-neutral zone of the solution, which reflects the surface charge of particles with a corresponding counter ion, is known as the zeta potential (Vinogradova et al., 2020). In nano-dispersion, the zeta potential denotes the strength of the attraction between nearby charged particles (Bhattacharjee, 2016). All the used excipients in this study were non-ionic; however, the zeta potential results shows that the surface of the droplets is negative due to the presence of fatty acid in oils (McNaught and Wilkinson, 1997). The zeta potential high negative values for the prepared NE formulas means that the repulsion forces exceed the attractive forces between the NE droplets. This will keep the system deflocculated state and the droplets remain dispersed without tendency for aggregation (McClements et al., 2022).

The drug EE of the formulas was found to be high and within the accepted limit which indicated that the choice of components, their concentrations and ratios as well as the procedure applied were efficient (Sun et al., 2012).

All the NE were colored orange by the dye indicating that the external phase is water and the NE of o/w type (McClements, 2002).

The electrical conductivity (EC; σ) of the formulated lomustine NE was determined to identify the nature or type of the NE external phase. This test values depends on the water higher conductivity in comparison to oil, therefore give high electrical conductivity for o/w NE where the external phase is water. All the results or measurements (Table 3) indicated that all the prepared NE were o/w type due to the high electrical conductivity (241–998 μs/cm). The higher NE conductivity affected by the percent of water where the formulas with lowest electrical conductivity had lowest water content (F16 of 35% and F7 of 30%) since larger water content let more freedom for ions mobility (Kalra et al., 2010).

The dilution test of the 18 formulas showed clear NE in less than one min indicated that the NE formulations were stable o/w type (Beg et al., 2013).

The transmittance test values of close 100% (Table 3) referred to the tiny size of droplet of all NE formulas and that what makes them transparent (Sarkar and Hardenia, 2011).

All the pH values of the formulated NE was within the acceptable pH range values of the nasal cavity which usually can tolerate formulations pH range of 3–10 (Jagdale et al., 2016).

The formulas (F5-F9 and F12-F18) that containing Transcutol P as a co-surfactant in Smix mixture showed the lowest viscosity. Formulas F9 (containing 40% Triton X-100:Transcutol P Smix in 2:1 ratio) has lowest viscosity between the others because it has high Transcutol P percentages (13.33%) and only 26.6% Triton X-100 (the viscous surfactant).

The highest viscosity was observed with formulas that containing Cremophore El (F1-F4, F10 and F11), formula F1 (containing 40% Triton X-100:Cremophore El Smix in 3:1 ratio) and F3 (containing 50% Triton X-100:Cremophore El Smix in 2:1 ratio) showed highest viscosity since they contain the higher percentage of Cremophore El (cosurfactant; viscous liquid) as well as high percentage of Triton X-100. Upon changing the co-surfactant to Transcutol P (with lowest viscosity), the NE formulas (F5-F9 and F12-F18) containing Triton X-100:Transcutol P Smix gave lower viscosity. The viscosity was directly related to the Smix percentage in the NE formulations. Similar observation was found with Isradipine (Ghareeb, 2020) and norcanthridin (Zeng et al., 2019) NE prepared using Transcutol P or Cremophore El, respectively.

All NE formulas had no separation or creaming after subjected to the physical tests (centrifugation, heating/cooling, and freeze/thaw cycle) indicating their physical stability (Shaikh et al., 2019).

The effect of using different amount of oil on drug release (Fig. 3A) showed that F11 (containing 5% oil) gave 100% drug release within 60 min which was significantly ($p \leq 0.05$) higher than F4 (containing 10% oil) which gave 100% release within 90 min. This could be attributed to the smaller droplet size of F11 (43.48 nm) which provided larger surface area that enhanced drug dissolution and caused fast passage and high diffusion of the drug through dialysis membrane (Sun et al., 2012; Jaiswal et al., 2015). For formulas F6 (containing 10% oil) and F15 (containing 5% oil), both having similar release profile (f_2 = 50.74) but F6 gave 100% release within 45 min while F15 reach 100% drug release within 60 min due to smaller droplet size of F6 (14.4 nm) in comparison to F15 (66.2 nm). Similar results observed with limonene NE which had small droplet size and gave faster dissolution (Hidajat et al., 2020).

Fig. 3B shows the effect of co-surfactant type, where F2 (containing 30% Triton X-100: Cremophore El in 3:1 ratio) gave 100% drug release within 90 min which was significantly ($p \leq 0.05$) lower than F6 (containing 30% Smix with Transcutol P instead of Cremophore El in 3:1 ratio) that gave 100% release within 45 min. Same scenario was with F15 (containing 30% Triton X-100: Transcutol P in a ratio of 3:1) gave 100% lomustine release within 45 min that was significantly ($p \leq 0.05$) faster than F10 (containing 30% Smix with Cremophore El as co-surfactant instead of Transcutol) which gave 100% release within 90 min. This could be due to the smaller droplet size of F6 (14.4 nm) and F15 (66.2 nm) in comparison to F2 (99.12 nm) and F10 (78 nm) which gave larger surface area then better dissolution for the drug, beside the lower viscosity of F6 (30.1 mPa.s) and F15 (26.3 mPa.s) since both containing the low viscous co-surfactant (Transcutol P) which facilitate the drug dissolution and release from the NE through the dialysis membrane. Similar observation was obtained with Itraconazole NE (Malik et al., 2022).

Fig. 3C shows the effect of Smix percentage on drug release, where formula F1 (containing 40% Smix) gave faster release of 100% drug within 15 min in comparison with F2 (containing 30% Smix; both of them containing 10% oil and same Smix; Triton X-100: Cremophore El at ratio; 3:1) which needed 90 min to release 100% of its loaded drug. Formulas F3 (containing 50% Smix in comparison with F4 of 30% Smix (containing same Smix; Triton X-100: Cremophore El at ratio; 2:1) where F3 gave significantly higher drug release in the first 45 min. Finally, F7 NE formula (containing 60% Triton X-100: Transcutol P in a ratio of; 2:1) gave 100% drug release within 45 min which was significantly ($p \leq 0.05$) higher than F8 (containing 50% of the same Smix and ratio), where increasing the Smix percentage led to faster release of drug loaded in the formulated NE due to increase in effective interfacial area of the drug particles which exposed to dissolution media (phosphate buffer saline pH 6.4), then higher dissolution rate and rapid drug release as well as to the solubilizing effect of Smix (El-Laithy, 2008). Similar observation was found with paclitaxel NE (Chen et al., 2017). However, formulas F13 (containing 50% Smix) and F14 (with 40% same Smix) gave similar release pattern (f_2 = 58.79) and both reach 90% drug release in 45 min. This could be due to smaller droplet size of F14 nanoemulsion formulas (13.93 nm) than F13 (73.7 nm). Additionally, the lower viscosity of F14 (56.8 mPa.s) while F13 (101.3 mPa.s) which facilitied its drug release.

Fig. 3D shows the effect of Smix ratio on drug release. Where formula F11 (containing 30% Triton X-100: Cremophore El in a ratio of 2:1) gave 100% drug release within 60 min which was higher than F10 (containing 30% Triton X-100: Cremophore El in a ratio of 3:1)

which gave 100% drug release within 90 min. This could be attributed to the smaller droplet size of F11 (43.48 nm) in comparison to F10 (78 nm) which facilitate drug dissolution and release. Formula F7 (containing 60% Triton X-100: Transcutol P in a ratio of 2:1) gave 100% drug release within 45 min which was significantly ($p \leq 0.05$) higher than F5 (containing 60% Triton X-100: Transcutol P in a ratio of 3:1) and this could be due to the low viscosity of F7 because it contained higher percentage of Transcutol P than F5. Formula F16 (containing 60% Triton X-100: Transcutol P in a ratio of 2:1) gave 100% drug release within 30 min that was significantly ($p \leq 0.05$) faster than F12 (containing 60% Triton X-100: Transcutol P in a ratio of 3:1). This could be attributed to the smaller droplet size of F16 (10.78 nm). Therefore, the suitable 2:1 Smix ratio gave faster drug release, this indicated that 2:1 Smix ratio provided the suitable HLB value for the production of NE of smaller droplet size. However, F17 (containing 50% Triton X-100: Transcutol P in a ratio of 2:1) and F13 (containing 50% Triton X-100: Transcutol P in a ratio of 3:1) needed 90 min to release 100% of drug. Formula F18 (containing 40% Triton X-100: Transcutol P in a ratio of 2:1) gave 100% drug release within 90 min that significantly ($p \leq 0.05$) lower than F14 (containing 40% Triton X-100: Transcutol P in a ratio of 3:1) that gave 100% drug released within 45 min. Such results revealed that there are many factors should be taken in consideration in the formulation of a suitable NE.

Fig. 4 shows the rest formulas that mainly their drug release affected by viscosity. Where formula F18 (containing 5% oil) gave 90% lomustine release within 90 min while F9 (containing 10% oil) which gave 100% release within 60 min, in spite of the smaller size of F18 (10.81 nm) than F9 (13.05 nm). This could be due to lower viscosity of F9 (23.6 mPa.s) that facilitate drug permeation via dialysis membrane. Additionally, F5 formula (containing 60% Triton X-100: Transcutol P in ratio of 3:1) gave 100% drug release within 90 min, while F6 (containing 30% of the same Smix type and ratio) gave 100% release within 45 min as the viscosity of F6 (30.1 mPa.s) was lower than that of F5 (112.8 mPa.s). All these three formulas gave approximately the same release profile as they all had Transcutol P as co-surfactant and a smaller droplet size (less than 15 nm) (Kumar et al., 2008). Such contribution of viscosity of NE on drug release was also observed with budesonide NE (Prasad and Hari, 2021).

4.4. Selection of the optimized formula

Formula F1 was selected as the best lomustine nanoemulsion formula based on the results obtained including the small droplet size of 31.31 nm, low PDI of 0.159, high zeta potential of −30.65, appropriate pH (5.12), good electrical conductivity (951 µs/cm), elegant % T (99.08%), and lomustine content (98.12%). Moreover, it demonstrated faster in vitro release profile (100% release within 15 min).

4.5. Tem of the optimum nanoemulsion formula

The TEM Fig. 5 showed compatibility between the particle size analyser and TEM results as the size shown in the figure close to the analyser.

4.6. Fourier transform infrared spectroscopy

The results showed no negligible variations between the peaks of pure drug and optimum formula peaks. This indicating there was no interaction between the drug and the used excipients (Nandiyanto et al, 2019).

5. Conclusion

The aforementioned findings suggested that NE technology can be used in the formulation of lomustine for targeting brain cancer via nose-to-brain delivery. The produced NE exhibits acceptable properties as nanocarrier with a fast rate and complete drug release. Thus, it might help to increase drug permeability and, in turn, its absorption into systemic circulation, which can skip liver metabolism, reduce the drug toxicity and potentially increase targeting to the brain.

Declaration of Competing Interest

The authors declare that they have no known competing financial interests or personal relationships that could have appeared to influence the work reported in this paper.

Acknowledgment

The authors would like to thank Mustansiriyah University (www.uomustansiriyah.edu.iq) for supporting this work. Thanks are extended to Al-Farahidi University (www.uoalfarahidi.edu.iq) for its support.

References

Abdulkarim, M.F., Abdullah, G.Z., Chitneni, M., et al., 2010. Formulation and characterization of palm oil esters based nano-cream for topical delivery of piroxicam. Int. J. Drug Delivery. 2.
Algahtani, M.S., Ahmad, M.Z., Ahmad, J., 2022. Investigation of factors influencing formation of nanoemulsion by spontaneous emulsification: impact on droplet size, polydispersity index, and stability. Bioengineering 9, 384.
Ali, M.S., Alam, M.S., Alam, N., et al., 2014. Preparation, characterization and stability study of dutasteride loaded nanoemulsion for treatment of benign prostatic hypertrophy. Iranian J. Pharmaceut. Res: IJPR. 13, 1125.
Al-Tamimi, D.J., Hussein, A.A., 2021. Formulation and characterization of self-microemulsifying drug delivery system of tacrolimus. Iraqi J. Pharmaceut. Sci. 30, 91–100 (P-ISSN 1683-3597 E-ISSN 2521-3512).
Ankith, K., Reddy, B., Niranjan, B., 2013. Design, development and evaluation of novel a nanoemulsion of simvastatin. Int. J. Adv. Pharm. 3, 94–101.
Ashoor, J.A., Ghareeb, M.M., Formulation and In-vitro Evaluation of Methotrexate Nanoemulsion using Natural Oil.
Beg, S., Jena, S.S., Patra, C.N., et al., 2013. Development of solid self-nanoemulsifying granules (SSNEGs) of ondansetron hydrochloride with enhanced bioavailability potential. Colloids Surf. B Biointerfaces 101, 414–423.
Bhattacharjee, S., 2016. DLS and zeta potential–what they are and what they are not?. J. Control. Release 235, 337–351.
Chaudhari, P.M., Kuchekar, M.A., 2018. Development and evaluation of nanoemulsion as a carrier for topical delivery system by box-behnken design. Asian J. Pharm. Clin. Res. 11, 286–293.
Chen, L., Chen, B., Deng, L., et al., 2017. An optimized two-vial formulation lipid nanoemulsion of paclitaxel for targeted delivery to tumor. Int. J. Pharm. 534, 308–315.
Chen, W.-Z., Zhao, H.-F., Yang, L.-H., 2013. Outline for British Pharmacopoeia 2013. Chinese J. Pharmaceut. Anal. 33, 709–715.
Çınar, K., 2017. A review on nanoemulsions: preparation methods and stability. Trakya Üniversitesi Mühendislik Bilimleri Dergisi.
Delmas, T., Piraux, H., Couffin, A.-C., et al., 2011. How to prepare and stabilize very small nanoemulsions. Langmuir 27, 1683–1692.
Deore, S.K., Surawase, R.K., Maru, A., 2019. Formulation and evaluation of o/w nanoemulsion of ketoconazole. Res. J. Pharmaceut. Dosage Forms Technol. 11, 269–274.
Egan, R.W., 1976. Hydrophile-lipophile balance and critical micelle concentration as key factors influencing surfactant disruption of mitochondrial membranes. J. Biol. Chem. 251, 4442–4447.
El-Laithy, H.M., 2008. Self-nanoemulsifying drug delivery system for enhanced bioavailability and improved hepatoprotective activity of biphenyl dimethyl dicarboxylate. Curr. Drug Deliv. 5, 170–176.
Ganta, S., Talekar, M., Singh, A., et al., 2014. Nanoemulsions in translational research—opportunities and challenges in targeted cancer therapy. AAPS PharmSciTech 15, 694–708.
Ghareeb, M.M., 2020. Formulation and characterization of isradipine as oral nanoemulsion. Iraqi J. Pharmaceut. Sci. 29, 143–153 (P-ISSN: 1683-3597, E-ISSN: 2521-3512).
Ghosh, V., Mukherjee, A., Chandrasekaran, N., 2013. Ultrasonic emulsification of food-grade nanoemulsion formulation and evaluation of its bactericidal activity. Ultrason. Sonochem. 20, 338–344.

Gupta, A., Eral, H.B., Hatton, T.A., et al., 2016. Nanoemulsions: formation, properties and applications. Soft Matter 12, 2826–2841.
Gurpreet, K., Singh, S., 2018. Review of nanoemulsion formulation and characterization techniques. Indian J. Pharm. Sci. 80, 781–789.
Gustafson, D.L., Page, R.L., 2013. Cancer chemotherapy. Withrow MacEwen's Small Animal Clin. Oncol., 157–179.
Hanif, F., Muzaffar, K., Perveen, K., et al., 2017. Glioblastoma multiforme: a review of its epidemiology and pathogenesis through clinical presentation and treatment. Asian Pac. J. Cancer Prev. 18, 3.
Hidajat, M.J., Jo, W., Kim, H., et al., 2020. Effective droplet size reduction and excellent stability of limonene nanoemulsion formed by high-pressure homogenizer. Colloids Interf. 4, 5.
Hussein, A.A., 2014. Preparation and evaluation of liquid and solid self-microemulsifying drug delivery system of mebendazole. Iraqi J. Pharmaceut. Sci. 23, 89–100 (P-ISSN: 1683-3597, E-ISSN: 2521-3512).
Islam, S.U., Shehzad, A., Ahmed, M.B., et al., 2020. Intranasal delivery of nanoformulations: a potential way of treatment for neurological disorders. Molecules 25, 1929.
Jagdale, S., Shewale, N., Kuchekar, B.S., 2016. Optimization of thermoreversible in situ nasal gel of timolol maleate. Scientifica. 2016.
Jaiswal, M., Dudhe, R., Sharma, P., 2015. Nanoemulsion: an advanced mode of drug delivery system. 3 Biotech 5, 123–127.
Jang, J.-H., Jeong, S.-H., Lee, Y.-B., 2020. Enhanced lymphatic delivery of methotrexate using W/O/W nanoemulsion: In vitro characterization and pharmacokinetic study. Pharmaceutics 12, 978.
Jin, Y., Liu, D., Hu, J., 2021. Effect of surfactant molecular structure on emulsion stability investigated by interfacial dilatational rheology. Polymers 13, 1127.
Józsa, L., Vasvári, G., Sinka, D., et al., 2022. Enhanced antioxidant and anti-inflammatory effects of self-nano and microemulsifying drug delivery systems containing curcumin. Molecules 27, 6652.
Kalra, R., Mulik, R., Badgujar, L., et al., 2010. Development and characterization of microemulsion formulations for transdermal delivery of aceclofenac: a research. Int. J. Drug. Form. Res. 1, 359–386.
Khan, B.A., Akhtar, N., Khan, H.M.S., et al., 2011. Basics of pharmaceutical emulsions: A review. Afr. J. Pharm. Pharmacol 5, 2715–2725.
Klang, V., Matsko, N.B., Valenta, C., et al., 2012. Electron microscopy of nanoemulsions: an essential tool for characterisation and stability assessment. Micron 43, 85–103.
Kumar, S.V., Sasmal, D., Pal, S.C., 2008. Rheological characterization and drug release studies of gum exudates of Terminalia catappa Linn. AAPS PharmSciTech 9, 885–890.
Lai, S.K., Wang, Y.-Y., Hanes, J., 2009. Mucus-penetrating nanoparticles for drug and gene delivery to mucosal tissues. Adv. Drug Deliv. Rev. 61, 158–171.
Li, X., Anton, N., Ta, T.M.C., et al., 2011. Microencapsulation of nanoemulsions: novel Trojan particles for bioactive lipid molecule delivery. Int. J. Nanomed. 6, 1313.
Lundy, D.J., Nguy n, H., Hsieh, P.C., 2021. Emerging nano-carrier strategies for brain tumor drug delivery and considerations for clinical translation. Pharmaceutics 13, 1193.
Malik, M.R., Al-Harbi, F.F., Nawaz, A., et al., 2022. Formulation and characterization of chitosan-decorated multiple nanoemulsion for topical delivery in vitro and ex vivo. Molecules 27, 3183.
Mathew, D.S., Juang, R.-S., 2007. Role of alcohols in the formation of inverse microemulsions and back extraction of proteins/enzymes in a reverse micellar system. Sep. Purif. Technol. 53, 199–215.
McClements, D.J., 2002. Colloidal basis of emulsion color. Curr. Opin. Colloid Interface Sci. 7, 451–455.
McClements, D.J., Lu, J., Grossmann, L., 2022. Proposed methods for testing and comparing the emulsifying properties of proteins from animal, plant, and alternative sources. Colloids Interfaces 6, 19.
McNaught, A.D., Wilkinson, A., 1997. Compendium of Chemical Terminology. Blackwell Science Oxford.
Mota Ferreira, L., Gehrcke, M., Ferrari Cervi, V., et al., 2016. Pomegranate seed oil nanoemulsions with selective antiglioma activity: optimization and evaluation of cytotoxicity, genotoxicity and oxidative effects on mononuclear cells. Pharm. Biol. 54, 2968–2977.
Muzaffar, F., Singh, U., Chauhan, L., 2013. Review on microemulsion as futuristic drug delivery. Int. J. Pharm. Pharm. Sci. 5, 39–53.
Nan, A., 2015. Miscellaneous drugs, materials, medical devices and techniques. Side Effects of Drugs Annual, vol. 37. Elsevier, pp. 603–619.
Nandiyanto, A.B.D., Oktiani, R., Ragadhita, R., 2019. How to read and interpret FTIR spectroscope of organic material. Indonesian J. Sci. Technol. 4, 97–118.
Orafidiya, L.O., Oladimeji, F., 2002. Determination of the required HLB values of some essential oils. Int. J. Pharm. 237, 241–249.
Patel, K., Sarma, V., Vavia, P., 2013. Design and evaluation of lumefantrine–oleic acid self nanoemulsifying ionic complex for enhanced dissolution. DARU J. Pharmaceut. Sci. 21, 1–11.
Pouton, C.W., 1997. Formulation of self-emulsifying drug delivery systems. Adv. Drug Deliv. Rev. 25, 47–58.
Prajapati, S.T., Pathak, S.P., Thakkar, J.H., et al., 2015. Nanoemulsion based intranasal delivery of risperidone for nose to brain targeting. Bull. Pharmaceut. Res. 5, 6–13.
Prasad, K.L., Hari, K., 2021. Formulation and evaluation of solid self-nanoemulsifying drug delivery system for enhancing the solubility and dissolution rate of budesonide. Research J. Pharmacy Technol. 14, 5755–5763.
Raavi, S., Subramanian, S., Vuddisa, S., 2014. Supersaturated self nanoemulsifying tablets of atorvastatin. World J. Pharm. Pharm. Sci. 3, 1275–1286.
Rosen, P.L., Palmer, J.N., O'Malley Jr, B.W., et al., 2013. Surfactants in the management of rhinopathologies. Am. J. Rhinol. Allergy 27, 177–180.
Sarheed, O., Dibi, M., Ramesh, K.V., 2020. Studies on the effect of oil and surfactant on the formation of alginate-based O/W lidocaine nanocarriers using nanoemulsion template. Pharmaceutics. 12, 1223.
Sarkar, B., Hardenia, S., 2011. Microemulsion drug delivery system: for oral bioavailability enhancement of glipizide. J. Adv. Pharm. Educ. Res. 1, 195–200.
Sekeri, S.H., Ibrahim, M.N.M., Umar, K., et al., 2020. Preparation and characterization of nanosized lignin from oil palm (Elaeis guineensis) biomass as a novel emulsifying agent. Int. J. Biol. Macromol. 164, 3114–3124.
Shah, B.M., Misra, M., Shishoo, C.J., et al., 2015. Nose to brain microemulsion-based drug delivery system of rivastigmine: formulation and ex-vivo characterization. Drug Deliv. 22, 918–930.
Shaikh, N.M., Swamy, S.V., Narsing, N.S., et al., 2019. Formulation and evaluation of nanoemulsion for topical application. J. Drug Deliv. Therapeut. 9, 370–375.
Sharma, A., Singh, A., Harikumar, S., 2020. Development and optimization of nanoemulsion based gel for enhanced transdermal delivery of nitrendipine using box-behnken statistical design. Drug Dev. Ind. Pharm. 46, 329–342.
Shukla, S., Modi, D., Shah, D., 2016. A review on solid self-nanoemulsifying drug delivery system: an approach for bioavailability enhancement. World J Pharm Pharm Sci. 5, 302–316.
Sun, H., Liu, K., Liu, W., et al., 2012a. Development and characterization of a novel nanoemulsion drug-delivery system for potential application in oral delivery of protein drugs. Int. J. Nanomed. 7, 5529.
Sun, J., Wang, F., Sui, Y., et al., 2012b. Effect of particle size on solubility, dissolution rate, and oral bioavailability: evaluation using coenzyme Q10 as naked nanocrystals. Int. J. Nanomed. 7, 5733.
Vinogradova, O.I., Silkina, E.F., Bag, N., et al., 2020. Achieving large zeta-potentials with charged porous surfaces. Phys. Fluids 32, 102105.
Xi, J., Chang, Q., Chan, C.K., et al., 2009. Formulation development and bioavailability evaluation of a self-nanoemulsified drug delivery system of oleanolic acid. AAPS PharmSciTech 10, 172–182.
Zeng, L., Xin, X., Zhang, Y., 2017. Development and characterization of promising Cremophor EL-stabilized o/w nanoemulsions containing short-chain alcohols as a cosurfactant. RSC Adv. 7, 19815–19827.
Zeng, L., Liu, Y., Pan, J., et al., 2019. Formulation and evaluation of norcanthridin nanoemulsions against the Plutella xylostella (Lepidotera: Plutellidae). BMC Biotech. 19, 1–11.